Research Article

Drug Testing and Analysis

Received: 10 September 2008 Revised: 10 October 2008 Accepted: 10 October 2008 Published online in Wiley Interscience:

(www.drugtestinganalysis.com) DOI 10.1002/dta.8

Vibrational spectroscopic study of salbutamol hemisulphate

H. R. H. Ali,[1,3] H. G. M. Edwards,[1]* J. Kendrick[2] and I. J. Scowen[1]

Salbutamol hemisulphate is a relatively selective β_2-adrenergic agonist and is used as a bronchodilator. In this work, we present a detailed vibrational spectroscopic investigation of salbutamol hemisulphate using mid-infrared and near-infrared Fourier-transform (NIR-FT) Raman spectroscopies. These data are supported by quantum chemical calculations, which allow us to characterise the vibrational spectra of this compound reasonably. As such, this study could be viable for examining the way in which this drug interacts with its target molecules.

Keywords: Raman spectroscopy; infrared spectroscopy; salbutamol hemisulphate; β_2 agonist; quantum chemical calculations

Introduction

Salbutamol hemisulphate (SB) (synonym: albuterol hemisulphate) is a relatively selective β_2-adrenergic agonist used as a bronchodilator. Its chemical name (see Fig. 1)[1–4] is 1-(4-hydroxy-3-hydroxymethylphenyl)-2-(*tert*-butylamino) ethanol sulphate (2 : 1) (salt). Salbutamol hemisulphate is indicated for the prevention and relief of bronchospasm with reversible obstructive airway disease (asthma) and for the prevention of exercise-induced bronchospasm. It acts by stimulating the adenyl cyclase enzyme, which catalyses the formation of cyclic-3′, 5′-adenosine monophosphate (cyclic AMP) from adenosine triphosphate (ATP). The cyclic AMP thus formed mediates the cellular responses. The increased cyclic AMP levels are associated with relaxation of bronchial smooth muscles. Salbutamol hemisulphate is effective by both oral and inhalation routes of administration so it has been used in tablets, syrups, metered dose inhalers, and nebulised inhalation solutions.

Salbutamol hemisulphate, like other β_2- agonists, is misused by athletes for its potential to improve muscular strength via significant anabolic effects.[5] SB is often illegally used as a feed additive for its potential role in increasing muscular mass and reducing body fat in animal species.[6] However, SB is a steady substance, so it can be deposited easily in both human and edible animal tissues. When using at a higher dose or long term it is found to have severe poisoning side effects.[7] The misuse of SB by athletes has been demonstrated and banned by the World Anti-Doping Agency (WADA).[8] Its use as a feed additive for growth promotion in livestock growth, which has resulted in a number of reports of human food poisoning,[9] has also been prohibited in many countries.

Experimental vibrational spectroscopy is a simple and rapid analytical technique for determining the vibrations of molecular structures.[10] Theoretical vibrational frequency computations are sometimes used to support experimental results. They often using density functional theory (DFT).[11]

In this work, we record the infrared and near-infrared Fourier-transform (NIR-FT) Raman spectra of SB solid samples. These spectra were the starting point for a comprehensive vibrational study based on quantum chemistry DFT calculations. Theoretical data were used to give a reliable interpretation of the infrared and Raman spectra of SB.

Experimental

Materials

A specimen of SB was obtained from Sigma-Aldrich and used without further purification.

Raman spectroscopy

Fourier-transform Raman spectroscopy was carried out using a Bruker IFS 66 instrument with an FRA 106 Raman module attachment and a Nd^{3+}/YAG laser, operating at 1064 nm in the near infrared. The powdered specimens were examined in aluminium cups. The spectra were recorded at 4 cm^{-1} spectral resolution and 500 spectral scans accumulated to improve signal-to-noise ratios. Laser powers were maintained at 100 mW at the sample.

Infrared spectroscopy

The IR spectra were recorded as KBr discs (1 : 200) using a Digilab Scimitar 2000 series spectrometer. The spectra were recorded over the range of 650–4000 cm^{-1} at 4 cm^{-1} spectral resolution and the accumulation of 512 spectral scans.

All vibrational spectra were exported to the Galactic*. SPC format using GRAMS AI (Galactic Industries, Salem, NH, Version 8.0).

Calculation details

Calculations were performed on the SB cation using GAMESS-UK[12] and ORCA[13] quantum chemistry computer programs. The

* *Correspondence to: H. G. M. Edwards, Chemical and Forensic Sciences/University Analytical Centre, School of Life Sciences, University of Bradford, Bradford BD7 1 DP, UK. E-mail: h.g.m.edwards@bradford.ac.uk*

1 *Chemical and Forensic Sciences/University Analytical Centre, School of Life Sciences, University of Bradford, Bradford BD7 1 DP, UK*

2 *Institute of Pharmaceutical Innovation, University of Bradford, Bradford BD7 1DP, UK*

3 *Department of Pharmaceutical Analytical Chemistry, Faculty of Pharmacy, University of Assiut, Assiut, Egypt*

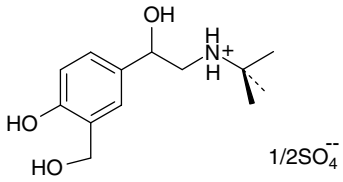

Figure 1. The chemical structure of salbutamol hemisulphate.

initial molecular cation structure used for geometry optimisation, using the BLYP density functional with a 6-31G* basis set,[14,15] was taken from Cambridge Crystal Structure Database (CSD) with code SALBUT. After geometry optimisation the infrared and Raman spectra were calculated within the quasiharmonic approximation, through diagonalisation of the mass-weighted Hessian matrix. Infrared and Raman intensities were calculated using the dipole-moment and polarisability derivatives of the normal modes.

Results and Discussion

The infrared and Raman spectra of SB were recorded over the wavenumber ranges 4000–600 cm^{-1} and 4000–100 cm^{-1} respectively, using both transmission and attenuated total reflectance modes of operation in the former and 1064 nm excitation wavelength in the latter.

The 3800–2200 cm^{-1} region

The infrared and FT-Raman spectra are shown in Fig. 2; these spectra demonstrate clearly the complexity of the structural information that is obtained from the vibrational analysis; the OH and NH stretching modes observed in the range 3500–3100 cm^{-1} in the infrared spectrum are not clearly observed in the Raman spectrum, whereas bands in the low wavenumber region that are normally characteristic of crystalline pharmaceutical forms are not recorded in the infrared spectrum. The observed infrared and Raman spectroscopic wavenumbers are listed in Table 1 along with the calculated values; assignment of the major experimental vibrational features was carried out in the light of the theoretical results and the vibrational spectroscopic data previously reported.[16–19] Several calculated modes have been matched with experimentally observed bands in the IR and Raman spectra, and these modes have been described; very weak features in the observed spectra cannot be reliably assigned on the basis of the theoretical calculations.

The broad, rather diffuse υ(OH) stretching band (Fig. 2) in the infrared spectrum at 3474 cm^{-1} suggests that hydrogen bonding occurs in the crystalline SB. The υ(NH) stretching band is observed in the infrared spectrum in the range 3280–3160 cm^{-1} (Fig. 2). The CH stretching region comprises several features in the wavenumber range 3130–2800 cm^{-1} (Fig. 2) for the infrared and Raman spectra); the CH stretching bands of the aromatic component of SB are shown in the Raman spectrum (Table 1) and can be assigned to the bands at 3127, 3107 and 3093 cm^{-1}. The CH aliphatic stretching bands of CH_3 symmetric and asymmetric stretching modes are shown in the both Raman and infrared spectra, and can be assigned to the medium strong features at 3025 and 2982 cm^{-1} and the medium feature at 2954 cm^{-1}in the infrared spectrum, the weak feature at 3027 cm^{-1}, the medium strong feature at 2985 cm^{-1}, the medium shoulder feature at 2973 cm^{-1} and the medium feature at 2880 cm^{-1} in the Raman spectrum. The broad medium band at 2927 cm^{-1} and the medium band at 2899 cm^{-1} in the Raman spectrum can be attributed to υ(CH) and $\upsilon(CH_2)$ attached to aliphatic (OH) respectively and the weak feature at 2623 cm^{-1} can be assigned to $\upsilon(CC)_{ring}$.

The 1800–1100 cm^{-1} region

This is a very important spectroscopic region for structural studies, particularly for the C═C group in this molecule. Expanded wavenumber regions of the infrared and Raman spectra are shown in Fig. 3. It is worth noting that the calculated band of $\delta(NH_2^+)$ at 1643 cm^{-1} was not observed in either the IR nor the Raman spectra and this may be attributed to the presence of sulphate anion, which may hinder this feature. The infrared region comprises a rich spectrum from the C═C functionality, along with several bands of medium and strong intensities, whereas the Raman spectrum consists mainly of the strong C═C features and several other weaker features. The υ(C═C) band occurs at 1616 cm^{-1}, of medium strong intensity in both the Raman and infrared spectra. The bands at 1616 and 1205 cm^{-1} in both Raman and infrared spectra and the bands at 1558 and 1205 cm^{-1} in the infrared spectrum can be assigned on the basis of quantum chemical calculations as hydrogen-bonded C–OH angle coupled to phenyl ring vibration. Again, it is worth noting that the calculated methyl

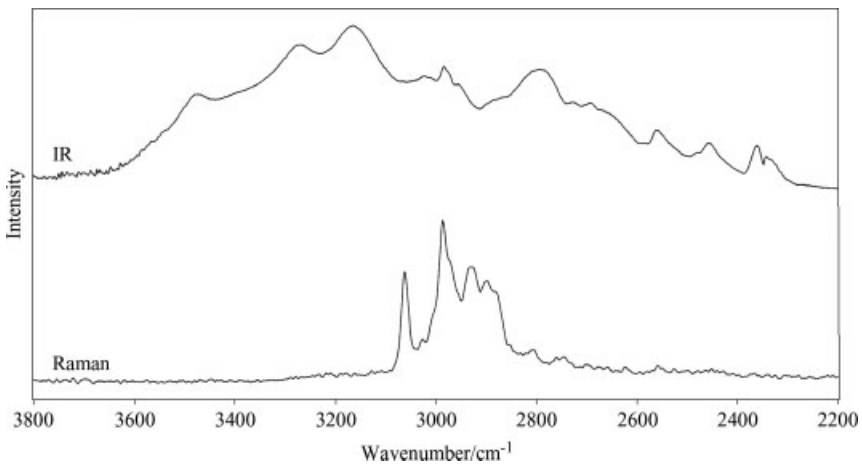

Figure 2. FT-Raman and IR spectral stack plot of SB in the 3800–2200 cm^{-1} region.

Table 1. The observed and calculated vibrational wavenumbers/cm^{-1} of SB. The calculated infrared intensities (I_{IR}) are relative to that of δ(COH) and δCH_2OH) at 1187 cm^{-1}. The calculated Raman intensities (I_{Raman}) are relative to that of $\upsilon_{as}(CH_3)$ at 2997 cm^{-1}

Observed		Calculated			
Raman (cm^{-1})	IR (cm^{-1})	υ	I_{Raman}	I_{IR}	Proposed assignment
	3474 ms	3573	0.450	0.250	υ(OH)
	3272 s	3344	0.158	0.141	υ(NH)
3190 vw					υ(NH)
3177 vw					υ(NH)
3160 vs	3162 s	3208	0.345	0.452	υ(NH)
3127 w		3120	0.384	0.504	$\upsilon(CH)_{ring}$
3107 vw		3103	0.255	0.335	$\upsilon(CH)_{ring}$
3093 vw		3091	0.400	0.057	$\upsilon(CH)_{ring}$
3062 m		3058	0.261	0.342	$\upsilon(CH_2)$ and $\upsilon(CH_3)$
3027 w	3025 ms	3037	0.235	0.308	$\upsilon_{as}(CH_2)$ attached to (OH)
2985 ms	2982 ms	2997	1.000	0.010	$\upsilon_{as}(CH_3)$
2973 m,sh		2992	0.115	0.046	$\upsilon_{as}(CH_3)$
	2954 m	2984	0.202	0.048	$\upsilon_{as}(CH_3)$
2927 br,m		2925	0.216	0.161	υ(CH) attached to aliphatic (OH)
2899 m		2920	0.622	0.237	$\upsilon(CH_2)$ attached to aliphatic (OH)
2880 m					$\upsilon(CH_3)$
2854 w					
2833 vw					
2821 vw					
2808 w,br					
	2793 ms,br				
2760 w					
2745 w,br					
2728 vw	2726 m				
2711 vw					
2702 w,br					
	2691 m				
2676 w					
2659 w					
2641 vw					
2623 w					$\upsilon(CC)_{ring}$
	2584 mw				
	2560 mw				
	2483 w				
	2457 mw				
	2360 mw				
	2341 w				
		1643	0.032	0.219	$\delta(NH_2^+)$
1616 ms	1616 ms	1625	0.259	0.177	Hydrogen bonded C–OH angle coupled to phenyl ring vibration and (C=C)
	1558 vw	1580	0.111	0.059	Hydrogen bonded C–OH angle coupled to phenyl ring vibration
		1569	0.036	0.052	$\delta(CH_3)$
		1563	0.069	0.172	$\delta(CH_3)$
		1552	0.033	0.027	$\delta(CH_3)$
	1539 vw	1527	0.014	0.391	$\upsilon(CC)_{ring}$
	1507 ms				$\delta(CH_2)_{(sciss.)}$
1494 mw		1489	0.062	0.031	
1468 m	1468 mw	1475	0.052	0.064	$\delta(CH_2\text{-}N)$
	1455 mw	1456	0.052	0.054	
	1438 m	1429	0.083	0.049	Ring stretch
	1409 mw	1419	0.029	0.183	Hydrogen bonded C–OH angle coupled to phenyl ring vibration
1395 vw	1395 m	1395	0.016	0.919	
	1386 m	1376	0.085	0.167	Mixed modes associated with $\delta(NH_2^+)$, $\delta(CH_2)$ and δ(CHOH)
	1379 m	1371	0.009	0.135	Mixed modes associated with $\delta(NH_2^+)$, $\delta(CH_2)$ and δ(CHOH)
1360 w	1362 mw	1355	0.076	0.038	Mixed modes associated with CH_2 and CH–OH vibrations

Table 1. (*Continued*)

Observed		Calculated			
Raman (cm^{-1})	IR (cm^{-1})	υ	I_{Raman}	I_{IR}	Proposed assignment
	1340 w	1344	0.006	0.290	Ring stretch
1331 vw					In-plane δ(CH)
	1309 vw	1299	0.028	0.014	
1283 vw		1290	0.009	0.119	υ(C-C) of the t- Butyl group
1255 m	1261 m, sh	1268	0.017	0.327	δ(CH)
	1244 m	1249	0.018	0.129	
1205 w	1205 m	1219	0.065	0.032	Hydrogen bonded C–OH angle coupled to phenyl ring vibration
1187 w					
1156 vw					υ(S=O)
	1126 ms, sh	1187	0.029	1.000	δ(COH) and $\delta(CH_2OH)$
	1112 vs	1106	0.031	0.141	Hydrogen bonded CH–OH angle coupled to phenyl ring vibration
1080 w	1084 s	1097	0.007	0.418	Hydrogen bonded CH–OH and CH_2OH angle coupled to phenyl ring vibration
1062 w	1060 ms	1067	0.017	0.008	
1034 vw	1029 vs	1033	0.014	0.124	r(CH_3)
1011 w	988 m	1012	0.060	0.446	υ_{as}(C–OH)
978 s	978 m	965	0.010	0.188	υ_{as}(C–OH)
	947 w	944	0.040	0.076	υ_{as}(C–OH)
937 mw		924	0.026	0.008	Out-of-plane δ(CH)
917 vw	916 mw	912	0.137	0.376	υ_{as}(CN)
881 w	882 w	910	0.073	0.102	$\delta(CH)_{ring}$
859 vw		869	0.026	0.074	$\delta(CC)_{ring}$
841 vw	840 m	835	0.041	0.121	υ_{as}(CN) attached to the quaternary carbon
	792 vw	796	0.013	0.137	Out-of-plane $\delta(CH)_{ring}$
780 ms	773 w	775	0.010	0.020	υ(C-C-O)
747 m	747 w	750	0.092	0.022	Ring vibration
729 vw		728	0.005	0.026	Out-of-plane $\delta(CC)_{ring}$
	668 w	670	0.003	0.006	CH wagging
648 w	647 w	651	0.006	0.006	CH wagging
609 vw	616 mw, sh	635	0.006	0.091	δ(CCC)
	610 m	593	0.006	0.066	Ring deformation
589 w		577	0.010	0.071	Out-of-plane $\delta(CCC)_{ring}$
569 vw	575 vw				In-plane δ(CCN)
533 w	534 w	520	0.033	0.011	Out-of-plane δ(CC)
487 mw	487 vw	472	0.009	0.014	
465 vw	464 w	457	0.002	0.124	$\delta(CC)_{chain}$
404 vw		409	0.017	0.664	δ(OH)
360 w		362	0.006	0.008	Out-of-plane (CCC) skeletal deformation
338 vw		333	0.004	0.126	Out-of-plane (CCC) skeletal deformation
312 w		318	0.013	0.250	In-plane (CCC) skeletal deformation
264 w		257	0.004	0.016	$CH_3\tau$
193 m		203	0.013	0.032	
165 ms		165	0.007	0.010	
150 ms		142	0.017	0.010	Skeletal mode
101 s		101	0.004	0.015	Skeletal mode
81 vs		92	0.001	0.015	Skeletal mode

deformation vibrational bands at 1569, 1563 and 1552 cm^{-1} have not been observed in the experimental spectra. This may be due to the presence of the sulphate anion, which may hinder the observation of some of the methyl deformation features. The very weak features at 1539 cm^{-1} and the medium/strong feature at 1507 cm^{-1} in the infrared spectrum can be assigned to $\upsilon(CC)_{ring}$ and $\delta(CH_2)_{(sciss.)}$ modes, respectively. The medium band in the Raman spectrum and the medium weak band in the IR spectrum at 1468 cm^{-1} can be assigned to $\delta(CH_2\text{-}N)$. In the 1390–1360 cm^{-1} range in the IR spectrum we have observed three bands at 1386, 1379 and 1362 cm^{-1}, which can be assigned on the basis of quantum chemical calculations as mixed modes associated with $\delta(NH_2^+)$, $\delta(CH_2)$ and δ (CHOH) groups. In the range 1470–1250 cm^{-1} we expect CH_3, CH_2 and CH aliphatic bending vibrations bands to occur. Lower in wavenumber, we have observed the υ(S=O) band at 1156 cm^{-1} in the Raman spectrum and the δ (COH) and $\delta(CH_2OH)$ bands at 1126 cm^{-1} and the very strong band at 1112 cm^{-1} in the IR spectrum, which can

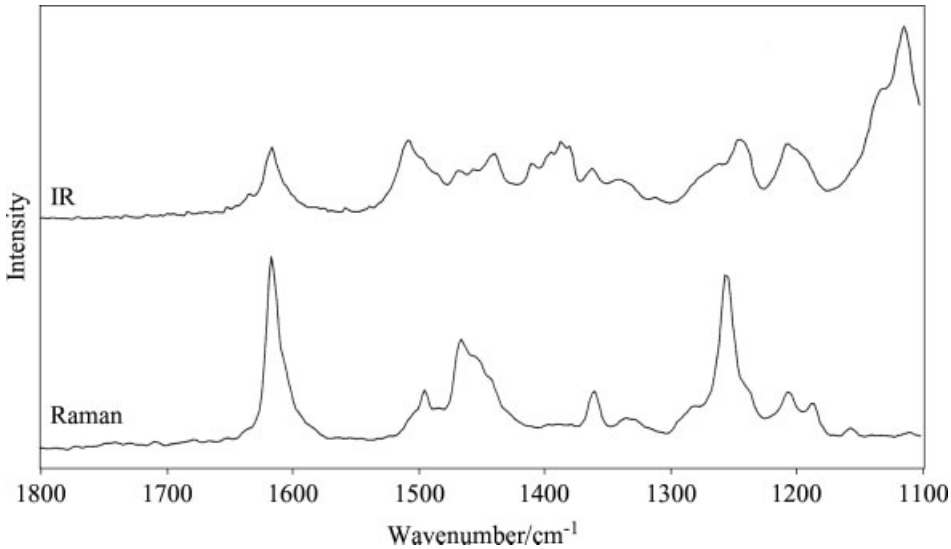

Figure 3. FT-Raman and IR spectral stack plot of SB in the 1800–1100 cm^{-1} region.

be assigned to the hydrogen-bonded CH–OH angle coupled to the phenyl ring vibration.

The 1100 cm^{-1} – 50 cm^{-1} region

Infrared and Raman spectra over this wavenumber range are presented in Fig. 4. The strong band in the IR spectrum at 1084 cm^{-1} can be assigned on the basis of quantum chemical calculation to hydrogen bonded CH–OH and CH_2OH angle coupled to phenyl ring vibration and the very strong band at 1029 cm^{-1} can be assigned to r(CH_3) mode. The three υ_{as}(C–OH) bands of the three primary OH groups of SB are more clearly shown in the IR spectrum of medium intensity at 988 and 978 cm^{-1} and weak intensity at 947 cm^{-1} as well as the υ_{as}(CN) and the υ_{as}(CN) attached to the quaternary carbon bands at 916 and 840 cm^{-1} respectively. Lower in wavenumber, we expect to find the υ(C-C-O) band at 780 cm^{-1} in the Raman spectrum and at 773 cm^{-1} in the IR spectrum and the CH wagging bands at 648 cm^{-1} in the Raman spectrum and at 668 and 647 cm^{-1} in the IR spectrum.

Finally, complex ring modes of CCC and CCN deformations in the range between 550 and 300 cm^{-1} occur. The very weak feature in the Raman spectrum at 404 cm^{-1} can be assigned on the basis of quantum chemical calculations to δ (OH). The methyl torsional band is observed in the Raman spectrum at 264 cm^{-1} of weak intensity. The skeletal mode extends over the region of 80 to 150 cm^{-1} in the Raman spectrum.

A good overall agreement was obtained between the experimental and calculated frequency values (Table 1); however, even with the support of quantum chemical calculations, it is difficult to be certain about some of these molecular vibration assignments especially in the mid-low wavenumber range because of the complexities of mode mixing. It is clear, however, that the major spectroscopic features of SB have been reasonably assigned in this study.

The key Raman spectral features of SB are the υ(NH) band at 3160 cm^{-1}, the υ(CH_2) and υ(CH_3) bands at 3062 cm^{-1}, the υ_{as}(CH_3) band at 2985 cm^{-1},the υ(CH) attached to aliphatic (OH)

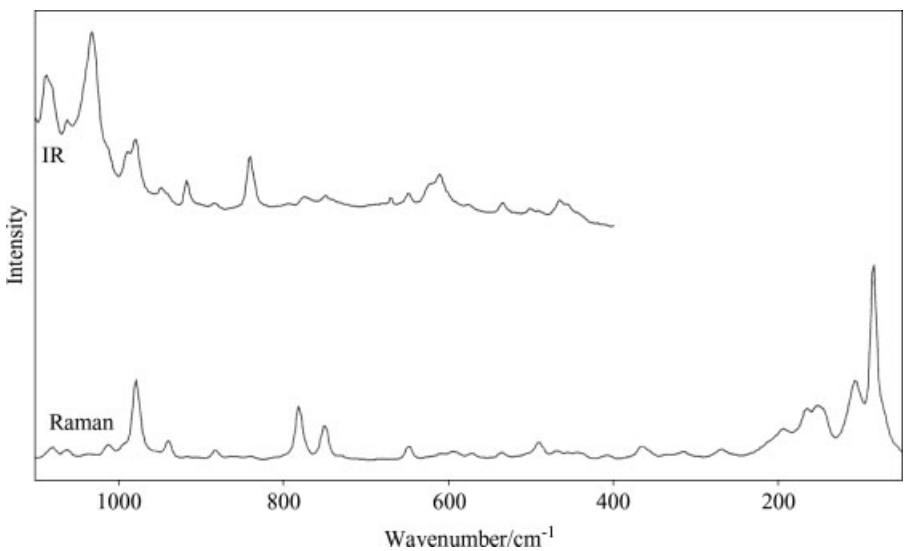

Figure 4. FT-Raman and IR spectral stack plot of SB in the 1100 cm^{-1} – 50 cm^{-1} region.

at 2927 cm^{-1}, the $\upsilon(CH_2)$ attached to aliphatic (OH) band at 2899 cm^{-1}, the $\upsilon(CH_3)$ band at 2880 cm^{-1}, the $\upsilon(C{=}C)$ band at 1616 cm^{-1}, the $\delta(CH_2\text{-}N)$ band at 1466 cm^{-1}, the $\delta(CH)$ band at 1255 cm^{-1}, and the $\upsilon_{as}(C{-}OH)$band at 978 cm^{-1}, the υ(C-C-O) band at 780 cm^{-1} and the skeletal mode bands at 150, 101 and 81 cm^{-1}, while its key infrared spectral features are the υ(OH) band at 3474 cm^{-1}, the υ(NH) bands at 3272 and 3162 cm^{-1}, the $\upsilon_{as}(CH_2)$ attached to (OH) band at 3025 cm^{-1}, the $\upsilon_{as}(CH_3)$ bands at 2982 and 2954 cm^{-1}, the $\upsilon(C{=}C)$ band at 1616 cm^{-1}, the $\delta(CH_2)_{(sciss.)}$ band at 1507 cm^{-1}, the mixed modes associated with $\delta(NH_2{}^+)$, $\delta(CH_2)$ and δ(CHOH) at 1386 and 1379 cm^{-1} the hydrogen-bonded C–OH angle coupled to phenyl ring vibration bands at 1205 and 1112 cm^{-1}, the hydrogen-bonded CH–OH and CH_2OH angle coupled to phenyl ring vibration bands at 1084 cm^{-1}, the r(CH_3) band at 1029 cm^{-1}, the υ_{as} (C–OH) bands of the three (OH) groups at 988, 978 and 947 cm^{-1} and the υ_{as}(CN) attached to the quaternary carbon band at 840 cm^{-1}.

Conclusions

Vibrational spectroscopy and quantum chemical calculations have been applied to the investigation of salbutamol hemisulphate. Raman and infrared spectra were recorded and the vibrational bands were assigned on the basis of the potential energy distribution obtained from the DFT calculations. As a result of the comparison of the experimental and calculated frequencies, the vibrational modes associated with the atoms involved in the hydrogen bonding were identified. These bands represent a powerful tool to investigate the possible polymorphic forms of salbutamol hemisulphate. As such, this study could be viable for examining the way in which this drug interacts with its target molecules.

Acknowledgement

Hassan R. H. Ali is grateful for the support of the government of the Arab Republic of Egypt during the period in which this work was carried out.

References

[1] M. Oliva, R. A. Olsina, A. N. Masi, *Analyst.* **2005**, *130*, 1312.
[2] Y. Yamini, C. T. Reimann, A. Vatanara, J. Å. Jönsson, *J. Cromatogr. A* **2006**, *1124*, 57.
[3] M. R. Ganjali, P. Norouzi, M. Ghorbani, A. Seperhi, *Talanta* **2005**, *66*, 1225.
[4] J. Zhang, Y. Xu, X. Di, M. Wu, *J. Cromatogr. B* **2006**, *831*, 328.
[5] P. M. Clarkson, H. S. Thompson, *Sports Med.* **1997**, *24*, 366.
[6] A. P. Moloney, P. Allen, T. V. McHugh, J. F. Quirke, *Livest. Prod. Sci.* **1995**, *42*, 23.
[7] V. Allister, *Medicine* **2007**, *35*, 597.
[8] www.wada-ama.org/ (accessed 2008).
[9] F. Ramos, A. Cristino, P. Carrola, T. Eloy, J. M. Silva, M. C. Castilho, M. I. N. Silveira, *Anal. Chim. Acta* **2003**, *483*, 207.
[10] H. R. H. Ali, H. G. M. Edwards, J. Kendrick, T. Munshi, I. J. Scowen, *J. Raman Spect.* **2007**, *38*, 903.
[11] B. I. Dunlap, *J. Chem. Phys.* **1983**, *78*, 3140.
[12] M. F. Guest, I. J. Bush, H. J. J. Van Dam, P. Sherwood, J. M. H. Thomas, J. H. Van Lenthe, R. W. A. Havenith, J. Kendrick, *Mol. Phys.* **2005**, *103*, 719.
[13] F. Neese. ORCA – An ab initio, density functional and semiempirical program package, version 2.4, revision 45, Max Planck Institut für Bioanorganische Chemie, Mülheim and der Ruhr, http://www.thch.uni-bonn.de/tc/orca/ **2005**, (accessed 2008).
[14] A. D. Becke, *Phys. Rev* **1988**, *A 38*, 3098.
[15] C. T. Lee, W. T. Yang, R. G. Parr, *Phys. Rev.* **1988**, *B 37*, 785.
[16] Electronic Handbook of FTIR Spectra. http://www.fdmspectra.com/fdm_ehb.htm (accessed 2008).
[17] A. B. Brown, P. York, A. C. Williams, H. G. M. Edwards, H. Worthington, *J. Pharm. Pharmacol.* **1993**, *45*, (suppl. 2): 1135.
[18] M. D. Ticehurst, R. C. Rowe, P. York, *Int. J. Pharm.* **1994**, *111*, 241.
[19] D. O. Corrigan, O. I. Corrigan, A. M. Healy, *Int. J. Pharm.* **2006**, *322*, 22.